Park et al., Biochem Pharmacol (Los Angel) 2016, 5:4
DOI: 10.4172/2167-0501.1000214

Biochemistry & Pharmacology: Open Access

Research Article Open Access

Induction of Activating Transcription Factor 6 via Activation of ERK and ROS-P38 MAPK is Related to Methylglyoxal-Induced Cytotoxicity in Human Retinal Pigment Epithelial Cells

Eun Jung Park[1], Young Sook Kim[1,2], Nu Ri Kang[1,2] and Jin Sook Kim[1,2]*

[1]Korean Medicine Convergence Research Division, Korea Institute of Oriental Medicine (KIOM), 1672 Yuseongdae-ro, Yuseong-gu, Daejeon, South Korea
[2]Korean Medicine Life Science, University of Science Technology (UST), 217 Gajeong-ro, Yuseong-gu, Daejeon, South Korea

Abstract

Methylglyoxal (MGO), a reactive α-oxoaldehyde produced by glucose metabolism, is elevated in several diabetic complications, including diabetic retinopathy. The breakdown of retinal pigment epithelial cells is implicated in the progression of diabetic retinopathy. Increased concentrations of MGO lead to retinal pigment epithelial cell death. In this study, we investigated the involvement of activating transcription factor 6 (ATF6) in MGO-mediated cytotoxicity in ARPE-19 cells. In response to high concentrations of MGO, unfolded protein response-related ATF6 was induced. Interestingly, the MGO also induced the generation of reactive oxygen species (ROS) and the phosphorylation of ERK and p38 MAPK. The induction of ATF6 was inhibited by ERK-specific and p38 MAPK-specific inhibitors (U0126 and SB202190) and by NAC, a well-known ROS scavenger. NAC also attenuated the phosphorylation of p38 MAPK. MGO induced cytotoxicity in the ARPE-19 cells, which was ameliorated by the inhibition of the ERK, p38 MAPK, and ROS pathways. Furthermore, the MGO-mediated cytotoxicity was inhibited by ATF6 siRNA. Taken together, these results clearly show that the induction of ATF6 via the ERK and ROS-p38 MAPK pathways is implicated in MGO-induced cytotoxicity in ARPE-19 cells.

Keywords: Diabetic retinopathy; Methylglyoxal; Activating transcription factor 6

Introduction

Diabetic retinopathy (DR), a major complication of diabetes, is a leading cause of vision loss among working-age adults in developed countries [1]. Recently, various structural and secretory dysfunctions of the retinal pigment epithelium (RPE) have been found in DR, and the breakdown of the RPE barrier plays a critical role in the induction of DR [2,3]. Therefore, the protection of the RPE is essential for retinal survival and, consequently, for visual function.

Methylglyoxal (MGO) is a highly reactive α-oxoaldehyde formed during glycolysis and generally metabolized by glyoxalase 1 (Glo-1) [4]. In diabetes, the chronic hyperglycemic condition induces the excessive formation of MGO [5]. MGO is major precursor of advanced glycation end products and has recently been shown to cause the induction of the receptor for advanced glycation end products [6,7]. Furthermore, the MGO-mediated accumulation of advanced glycation end products is closely correlated with DR [8].

The endoplasmic reticulum (ER) is a main organelle for protein synthesis and processing in eukaryotic cells [9]. ER stress, caused by the structural and functional disturbance of the ER, leads to the accumulation of misfolded or unfolded proteins and alterations in calcium homeostasis, triggering the unfolded protein response (UPR) [10]. Activating transcription factor 6 (ATF6) is one of the ER-resident UPR proteins. ATF6 is transported to the Golgi and processed by site-1 and site-2 proteases in response to stressful conditions [11]. Processed cytosolic ATF6 is translocated to the nucleus and controls the genes that encode ER-associated degradation components and XBP1 [12]. According to previous *in vivo* studies, ATF6 grains are observed in diabetic cataracts, and ATF6 is elevated in the retinal structures of db/db mice [13,14]. Also, ATF6 is induced by highly oxidized, glycated LDL in human retinal Müller cells, and ATF6 is translocated to the nucleus in retinal capillary pericytes [15,16]. However, there is no report on the role of ATF6 in eye disease, including DR. Therefore, we aimed to investigate the role of ATF6 in MGO-induced DR conditions in ARPE-19 cells.

Materials and Methods

Cell culture and reagents

ARPE-19 cells were obtained from the American Type Culture Collection (ATCC, Manassas, VA, USA). Cells were grown in Dulbecco's modified Eagle's medium/Ham's F-12 with 10% fetal bovine serum, 3 mM glutamine, and streptomycin/penicillin (100 mg/ml and 100 U/ml, respectively) in a 5% CO_2 incubator at 37°C. MGO and N-Acetyl-L-cysteine (NAC) were purchased form Sigma-Aldrich (St. Louis, MO, USA). SP600125, U0126, and SB202190 were obtained from Calbiochem (San Diego, CA, USA). Anti-ATF6 and actin antibodies were purchased from Santa Cruz Biotechnology (Santa Cruz, CA, USA). Anti-p-JNK, p-ERK, p-p38, JNK, ERK, and p38 antibodies were purchased from Cell Signaling Technology (Danvers, MA, USA).

Cell viability assay

The 3-(4,5-dimethylthiazol-2-yl)-2,5-diphenyltetrazolium bromide (MTT) assay was employed to measure cell viability. In brief, cells were

***Corresponding author:** Jin Sook Kim, Korean Medicine Convergence Research Division, Korea Institute of Oriental Medicine (KIOM), 1672 Yuseongdae-ro, Yuseong-gu, Daejeon 305-811, South Korea, Tel: 82-42-868-9465; Fax: 82-42-868-9471; E-mail: jskim@kiom.re.kr

Received May 31, 2016; **Accepted** July 08, 2016; **Published** July 15, 2016

Citation: Park EJ, Kim YS, Kang NR, Kim JS (2016) Induction of Activating Transcription Factor 6 via Activation of ERK and ROS-P38 MAPK is Related to Methylglyoxal-Induced Cytotoxicity in Human Retinal Pigment Epithelial Cells. Biochem Pharmacol (Los Angel) 5: 214. doi:10.4172/2167-0501.1000214

plated on 96-wll plates and incubated with various concentrations of MGO with or without inhibitors. At the appropriate time, 20 µl MTT solutions (5 mg/ml) was added to each well and incubated for 4 h at 37°C. After incubation, the MTT solution was removed, and 100 µl DMSO was added to each well. Absorbance at 570 nm was measured in a microplate reader (BIO-TEK, Synergy HT, Winooski, VT, USA).

Western blotting

Cells were lysed with Laemmli sample buffer (Bio-Rad, Hercules, CA, USA), heated at 100°C for 5 min, and electrophoresed at 20 µg/lane on a denaturing SDS–polyacrylamide gel. Proteins were transferred to nitrocellulose membranes (GE Healthcare UK Ltd, Buckinghamshire, Germany) using a Bio-Rad tank blotting apparatus (Bio-Rad). Membranes were probed with specific targeting primary polyclonal antibodies, washed, and incubated with horseradish peroxidase-linked secondary antibodies. After the membranes were washed three times, signals were detected using EzWestLumiOne (Atto Corporation, Tokyo, Japan) and Fugifilm LAS-3000 (LAS-3000, Fuji Photo, Tokyo, Japan).

Measurement of reactive oxygen species (ROS) generation

The generation of ROS was measured by using 2',7'-dichlorofluorescein diacetate (DCF-DA) as a substrate (Invitrogen, Carlsbad, CA, USA). In brief, cells were incubated with 10 µM DCF-DA for 30 min before collection. For quantitative assessment of ROS generation, the cells were collected, suspended in PBS, and analyzed by the green fluorescence intensity from 10,000 cells with a FACSCalibur flow cytometer (Becton Dickinson, Franklin Lakes, NJ, USA). For image taking, DCF-DA-loaded cells were visualized using an Olympus IX81 microscope (Olympus, Tokyo, Japan).

siRNA transfections

The ATF6 siRNA duplexes used in this study were purchased from Dharmacon as siGENEOME SMART pool M-009917-01 (Thermo Fischer Scientific, Pittsburgh, PA, USA). Cells were transfected with siRNA oligonucleotides using Oligofectamine Reagent (Invitrogen, Carlsbad, CA, USA) according to the manufacturer's recommendations.

Densitometry

The band intensities were quantified using the open source software ImageJ 1.50b (Image Processing and Analysis in Java; http://imagej.nih.gov/ij/).

Statistical analysis

The data were statically analyzed with a Student's t-test. A p-value <0.05 was considered significant (SPSS for Window, version 22.0, IBM, Armonk, NY, USA).

Results

MGO decreases cell viability and induces ATF6 up-regulation in ARPE-19 cells

Previous reports have shown that the ER stress pathway activates many diabetic complications including DR [17-19]. Also, various ER stress-related factors such as CHOP and ATF4 are involved in the progression of DR [16,20]. In this study, we aimed to investigate how ATF6 participates in MGO-induced DR in ARPE-19 cells. First, we treated ARPE-19 cells with MGO and observed the change in the expression level of ATF6 protein by using Western blotting. ATF6 protein expression levels were increased by 500 µM MGO (Figures 1A and 1B). MGO has cytotoxic activity as a well-known DR inducer [8]. To investigate the effect of MGO on cell viability in our system, ARPE-19 cells were treated with various concentrations (5-1000 µM) of MGO for 24 and 48 h. As shown in Figures 1C and 1D, cell viability was decreased by 500 and 1000 µM MGO, respectively. Furthermore, cell numbers were diminished, and morphological changes were also observed in the cells treated with 500 or 1000 µM MGO (Figure 1E).

Activation of ERK and p38 mediates MGO-induced ATF6 up-regulation and viability loss in ARPE-19 cells

According to several reports, the activation of MAPKs is involved in the induction of ATF6 [21-23]. We investigated the effect of MGO on MAPK phosphorylation in order to determine whether the activation of MAPKs is involved in MGO-induced ATF6 expression. The phosphorylation of JNK, ERK, and p38 peaked at 30 min after treatment with MGO (Figure 2A). Next, to test the role of individual MAPK pathways in MGO-induced ATF6 up-regulation and cytotoxicity, we examined the effects of SP600125 (an inhibitor of JNK), U0126 (an inhibitor of ERK), and SB202190 (an inhibitor of p38) on MGO-induced ATF6 expression and cell viability. As shown in Figure 2B, pre-treatment with U0126 and SB202190 slightly decreased the MGO-induced ATF6 up-regulation. However, SP600125, the JNK inhibitor, weakly increased ATF6 expression. Also, MGO-mediated cytotoxicity was partially restored by U0126 and SB202190 (Figure 2C). These results show that the induction of ATF6 and cytotoxicity might be partially mediated by the activation of the ERK and p38 signaling pathways in response to MGO in ARPE-19 cells.

ROS mediate MGO-induced ATF6 up-regulation and viability loss in ARPE-19 cells

MGO can generate ROS by reducing cellular glutathione levels [24]. To elucidate whether MGO generates ROS in ARPE-19 cells, the cells were incubated with DCF-DA, and relative green-fluorescence intensity was analyzed by flow cytometry and fluorescence microscopy. ROS were generated by 500 µM MGO in ARPE-19 cells (Figures 3A and 3B). To examine whether ROS generation might be involved in MGO-induced ATF6 expression in ARPE-19 cells, the cells were pre-treated with the ROS scavenger NAC and treated with MGO. ATF6 protein levels were then analyzed by Western blotting. As shown in Figure 3C, pre-treatment with NAC effectively suppressed MGO-induced ATF6. To further elucidate whether the ROS generation might participate in the activation of MAPK signaling pathways, cells were treated with NAC and MGO, and the phosphorylation states of ERK and p38 were subsequently checked. Interestingly, the MGO-induced phosphorylation of p38, but not that of JNK, was diminished by the NAC pre-treatment (Figure 3D). Furthermore, we tested the protective effect of NAC on the MGO-mediated reduction in cell viability. Pre-treatment with NAC completely ameliorated the MGO-mediated cytotoxicity (Figure 3D). Taken together, the results show that MGO-mediated ATF6 induction and viability reduction are induced by ROS and the activation of the p38 pathway in ARPE-19 cells.

ATF6 mediates MGO-induced cytotoxicity in ARPE-19 cells

To investigate how MGO-induced ATF6 regulates cell viability, ARPE-19 cells were transfected with control siRNA (siControl) and

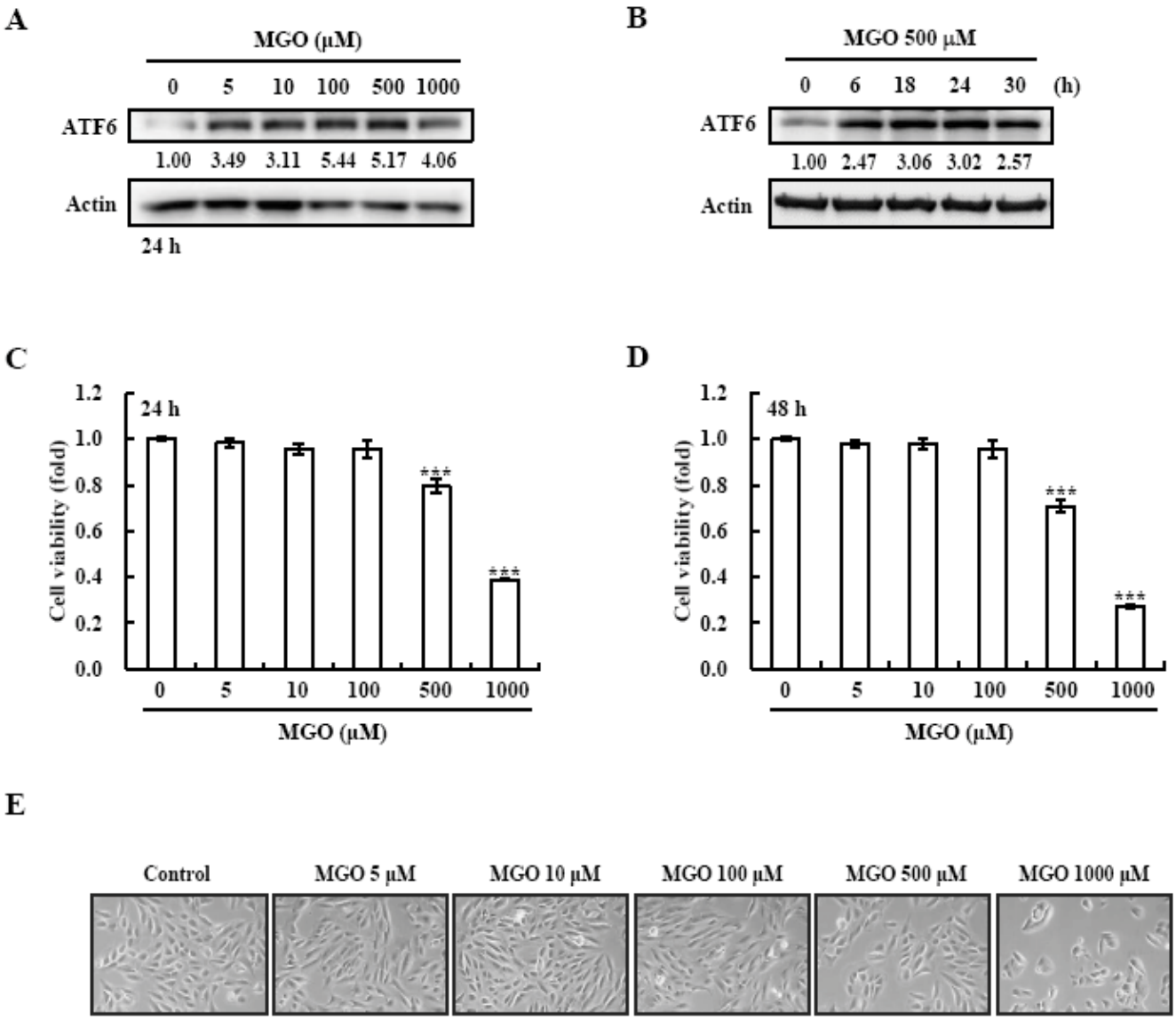

Figure 1: The effects of MGO on ATF6 protein expression levels, cell viability, and morphology in ARPE-19 cells. (A and B) ARPE-19 cells were seeded on 6-well culture plates and treated for 24 h with 5-1000 μM MGO or in a time-kinetic manner with 500 μM MGO, and the expression levels of ATF6 were observed by Western blotting. Actin served as a loading control. (C and D) ARPE-19 cells were seeded on 96-well culture plates and treated for 24 or 48 h with 5-1000 μM MGO, and cell viability was measured by MTT assay. (E) After treatment with 5-1000 μM MGO for 24 h, ARPE-19 cells were observed under an inverted microscope. Data are representative results from three independent experiments and expressed as mean ± SD. ***P<0.001 vs. control (n=8).

ATF6 siRNA (siATF6), and cell viability was measured in the presence or absence of MGO. A reduction in ATF6 protein level following transfection with siATF6 was identified by Western blotting (Figure 4A). MGO-mediated viability loss was partially ameliorated by the knockdown of ATF6 (Figure 4B). These result shows that the MGO-induced decrease in viability was mediated by ATF6 in ARPE-19 cells.

Discussion

In this study, we demonstrated for the first time that MGO induces cytotoxicity through the ERK-ATF6 and ROS-p38 MAPK-ATF6 pathways in ARPE-19 cells. The RPE is important for the maintenance of the visual system and is implicated in the pathogenesis of DR [2,3]. As a diabetic condition, a high concentration of MGO induces apoptosis and cytotoxicity [25-27]. Similarly, our data show decreased cell viability with an increased concentration of MGO (Figure 1). Because the balance between cell survival and death in the RPE is highly associated with DR, these result show that the loss of ARPE-19 cells due to the excessive accumulation of MGO might be associated with the progression of DR.

According to previous reports, the ER stress marker CHOP plays an important role in MGO-mediated myocyte apoptosis, and MGO induces the UPR through the phosphorylation of UPR proteins (PERK and eIF2a) in human lens epithelial cells [28,29]. Also, the ER stress pathway activates many diabetic complications including DR, and

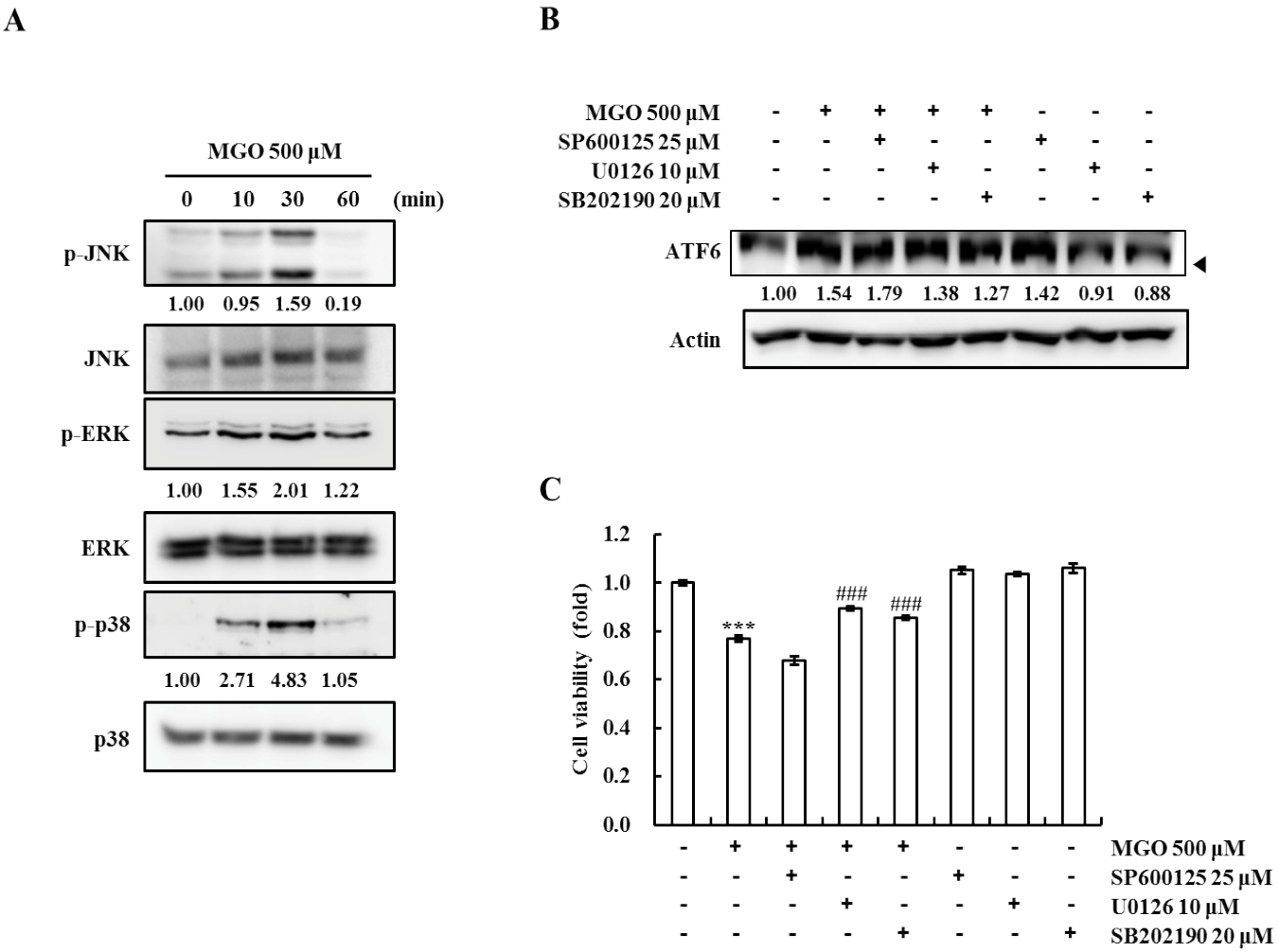

Figure 2: Involvement of MAPK pathways in MGO-mediated up-regulation of ATF6 and decreased viability in ARPE-19 cells. A) ARPE-19 cells were seeded on 6-well culture plates and treated for 10, 30, and 60 min with 500 μM MGO, and the phosphorylation levels of JNK, ERK, and p38 were determined by Western blotting using specific antibodies. The total form of JNK, ERK, and p38 served as a loading control. B) ARPE-19 cells were seeded on 6-well culture plates and treated for 24 h with 500 μM MGO in the presence or absence of JNK, ERK, and p38 inhibitors, and the expression levels of ATF6 were observed by Western blotting. C) ARPE-19 cells were seeded on 96-well culture plates and treated for 24 h with 500 μM MGO in the presence or absence of JNK, ERK, and p38 inhibitors, and cell viability was measured using the MTT assay. Data are representative results from three independent experiments and expressed as mean ± SD. $^{***}P<0.001$ vs. control; $^{###}P<0.001$ vs. MGO (n=8).

well-known ER stress-related factors (CHOP, ATF4, and GRP78/BiP) are involved in the progression of DR [16-20]. This is a novel finding that the induction of ATF6 occurs in MGO-treated RPE.

ER stress induces defense and restoration mechanisms using the UPR at early stages, but when the pro-survival UPR fails to overcome ER stress, it is sufficient to induce apoptosis and reduce cell viability [30]. Also, when ER stress is induced, ER-associated degradation is activated by ATF6, leading to cell survival, but ATF6 is also involved in the induction of cell death through the activation of pro-apoptotic CHOP [12,23,31-33]. Recent paper shows that MGO decreases RPE cell viability, resulting from the ER stress-dependent intracellular ROS formation, mitochondrial membrane potential loss, and intracellular calcium increase [34].

MAPK signaling is involved in the induction and activation of ATF6 [21-23]. In our data, the phosphorylation of JNK, ERK, and p38 MAPK was increased by MGO, but the induction of ATF6 was regulated by ERK and p38 MAPK (Figure 2). Furthermore, ROS generation is involved in cell death in several cell lines, and ROS generation is induced by MGO [5,7,24,27]. We also found that increased ROS were associated with the phosphorylation of p38, the induction of ATF6, and cytotoxicity in response to MGO in ARPE-19 cells (Figure 3). Therefore, the activation of ERK-ATF6 and ROS-p38-ATF6 by the excessive accumulation of MGO might be involved in the development of DR.

Conflict of Interest

The authors have no conflicts of interest to declare.

Acknowledgements

This research was supported by Grants (K16270) from the Korea Institute of Oriental Medicine (KIOM).

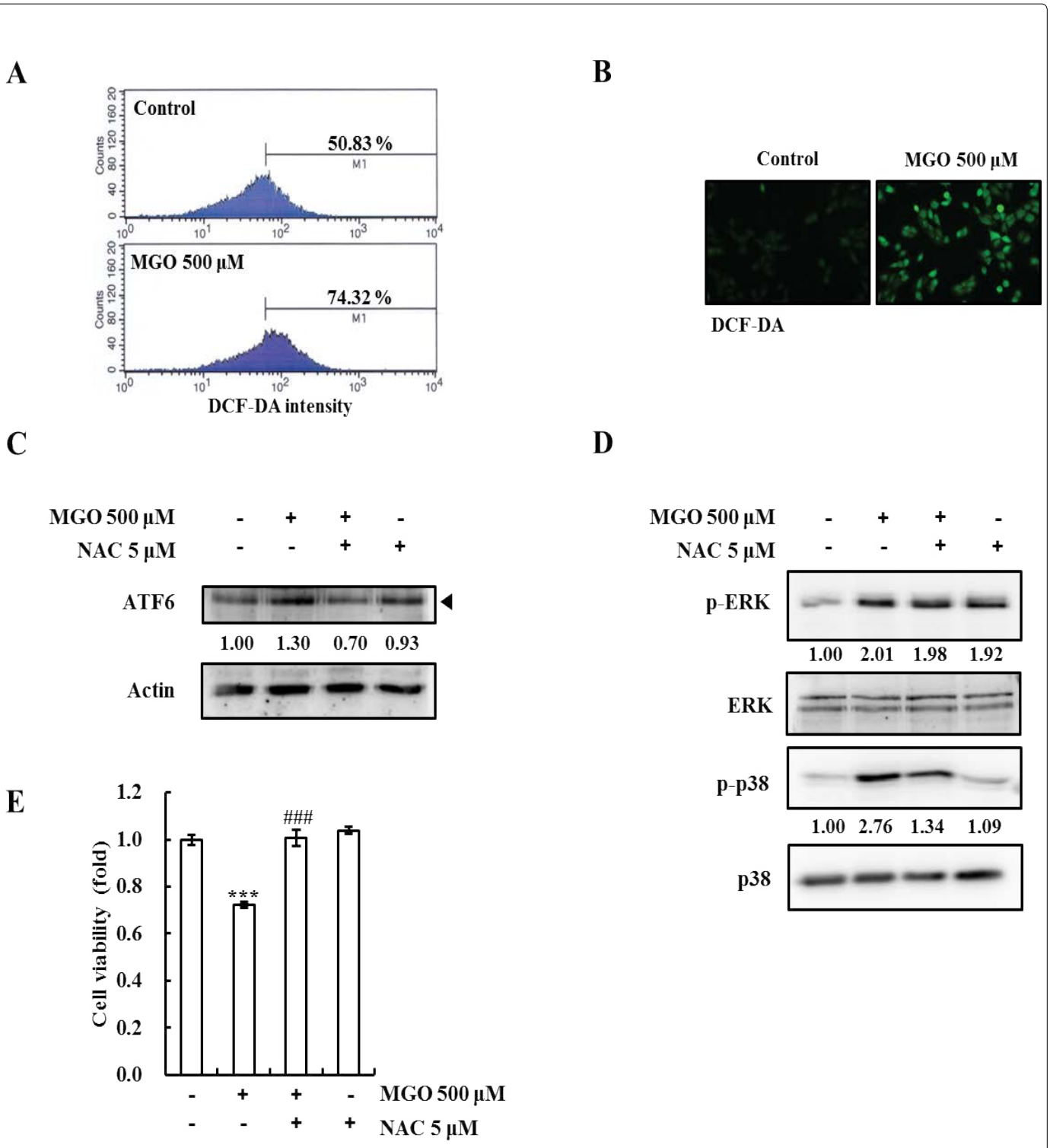

Figure 3: Involvement of ROS generation in MGO-mediated up-regulation of ATF6 and decreased viability in ARPE-19 cells. (A and B) ARPE-19 cells were seeded on 6-well culture plates and treated for 30 min with 500 µM MGO, and the DCF-DA-based ROS generation was determined using flow cytometry and fluorescence microscopy. C) ARPE-19 cells were seeded on 6-well culture plates and treated for 24 h with 500 µM MGO in the presence or absence of NAC, and the expression levels of ATF6 were observed by Western blotting. D) ARPE-19 cells were seeded on 6-well culture plates and treated for 30 min with 500 µM MGO, and the phosphorylation levels of ERK and p38 were determined by Western blotting. E) ARPE-19 cells were seeded on 96-well culture plates and treated for 24 h with 500 µM MGO in the presence or absence of NAC, and cell viability was measured by MTT assay. Data are representative results from three independent experiments and expressed as mean ± SD. $^{***}P<0.001$ vs. control; $^{###}P<0.001$ vs. MGO (n=8).

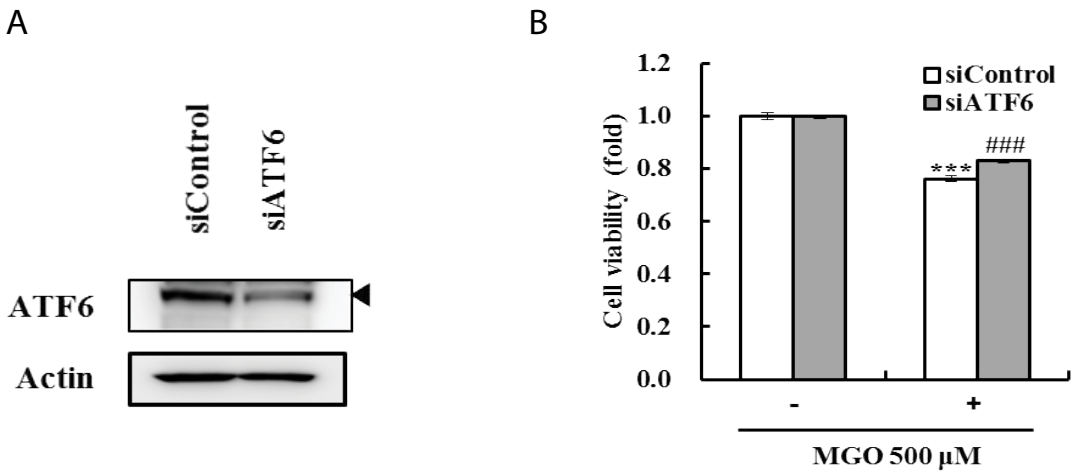

Figure 4: ATF6 is related to MGO-mediated decreased viability in ARPE-19 cells. (A and B) ARPE-19 cells were seeded on 6-well culture plates and transfected with control siRNA (siControl) or ATF6 siRNA (siATF6) with or without MGO after splitting. The cells were collected, the knockdown of ATF6 was observed by Western blotting, and cell viability was measured by MTT assay. Data are representative results from three independent experiments and expressed as mean ± SD. $^{***}P<0.001$ vs. control; $^{###}P<0.001$ vs. MGO (n=8).

References

1. Gargiulo P, Giusti C, Pietrobono D, La Torre D, Diacono D, et al. (2004) Diabetes mellitus and retinopathy. Dig Liver Dis 36: S101-S105.
2. Xu HZ, Song Z, Fu S, Zhu M, Le YZ (2011) RPE barrier breakdown in diabetic retinopathy: seeing is believing. J Ocul Biol Dis Infor 4: 83-92.
3. Simó R, Villarroel M, Corraliza L, Hernández C, Garcia-Ramírez M (2010) The retinal pigment epithelium: something more than a constituent of the blood-retinal barrier--implications for the pathogenesis of diabetic retinopathy. J Biomed Biotechnol 2010.
4. Piskorska D, Kopieczna-Grzebieniak E (1998) Participation of glyoxalases and methylglyoxal in diabetic complication development. Pol Merkur Lekarski 4: 342-344.
5. Thornalley PJ (1994) Methylglyoxal, glyoxalases and the development of diabetic complications. Amino Acids 6: 15-23.
6. Ramasamy R, Yan SF, Schmidt AM (2006) Methylglyoxal comes of AGE. Cell 124: 258-260.
7. Yao D, Brownlee M (2010) Hyperglycemia-induced reactive oxygen species increase expression of the receptor for advanced glycation end products (RAGE) and RAGE ligands. Diabetes 59: 249-255.
8. Stitt AW (2010) AGEs and diabetic retinopathy. Invest Ophthalmol Vis Sci 51: 4867-4874.
9. Hampton RY (2000) ER stress response: getting the UPR hand on misfolded proteins. Curr Biol 10: R518-R521.
10. Lindholm D, Wootz H, Korhonen L (2006) ER stress and neurodegenerative diseases. Cell Death Differ 13: 385-392.
11. Bernales S, Papa FR, Walter P (2006) Intracellular signaling by the unfolded protein response. Annu Rev Cell Dev Biol 22: 487-508.
12. Hetz C (2012) The unfolded protein response: controlling cell fate decisions under ER stress and beyond. Nat Rev Mol Cell Biol 13: 89-102.
13. Torres-Bernal BE, Torres-Bernal LF, Gutierrez-Campos RR, Kershenobich-Stalnikowitz DD, Barba-Gallardo LF, et al. (2014) Unfolded protein response activation in cataracts. J Cataract Refract Surg 40: 1697-1705.
14. Tang L, Zhang Y, Jiang Y, Willard L, Ortiz E, et al. (2011) Dietary wolfberry ameliorates retinal structure abnormalities in db/db mice at the early stage of diabetes. Exp Biol Med (Maywood) 236: 1051-1063.
15. Wu M, Yang S, Elliott MH, Fu D, Wilson K, et al. (2012) Oxidative and endoplasmic reticulum stresses mediate apoptosis induced by modified LDL in human retinal Muller cells. Invest Ophthalmol Vis Sci 53: 4595-4604.
16. Fu D, Wu M, Zhang J, Du M, Yang S, et al. (2012) Mechanisms of modified LDL-induced pericyte loss and retinal injury in diabetic retinopathy. Diabetologia 55: 3128-3140.
17. Oshitari T, Hata N, Yamamoto S (2008) Endoplasmic reticulum stress and diabetic retinopathy. Vasc Health Risk Manag 4: 115-122.
18. Ma JH, Wang JJ, Zhang SX (2014) The unfolded protein response and diabetic retinopathy. J Diabetes Res 2014: 160140.
19. Li B, Wang HS, Li GG, Zhao MJ, Zhao MH (2011) The role of endoplasmic reticulum stress in the early stage of diabetic retinopathy. Acta Diabetol 48: 103-111.
20. Chen Y, Wang JJ, Li J, Hosoya KI, Ratan R, et al. (2012) Activating transcription factor 4 mediates hyperglycaemia-induced endothelial inflammation and retinal vascular leakage through activation of STAT3 in a mouse model of type 1 diabetes. Diabetologia 55: 2533-2545.
21. Thuerauf DJ, Arnold ND, Zechner D, Hanford DS, DeMartin KM, et al. (1998) p38 Mitogen-activated protein kinase mediates the transcriptional induction of the atrial natriuretic factor gene through a serum response element. A potential role for the transcription factor ATF6. J Biol Chem 273: 20636-20643.
22. Luo S, Lee AS (2002) Requirement of the p38 mitogen-activated protein kinase signalling pathway for the induction of the 78 kDa glucose-regulated protein/immunoglobulin heavy-chain binding protein by azetidine stress: activating transcription factor 6 as a target for stress-induced phosphorylation. Biochem J 366: 787-795.
23. Tay KH, Luan Q, Croft A, Jiang CC, Jin L, et al. (2014) Sustained IRE1 and ATF6 signaling is important for survival of melanoma cells undergoing ER stress. Cell Signal 26: 287-294.
24. Beard KM, Shangari N, Wu B, O'Brien PJ (2003) Metabolism, not autoxidation, plays a role in alpha-oxoaldehyde- and reducing sugar-induced erythrocyte GSH depletion: relevance for diabetes mellitus. Mol Cell Biochem 252: 331-338.
25. Kim J, Son JW, Lee JA, Oh YS, Shinn SH (2004) Methylglyoxal induces apoptosis mediated by reactive oxygen species in bovine retinal pericytes. J Korean Med Sci 19: 95-100.
26. Fukunaga M, Miyata S, Liu BF, Miyazaki H, Hirota Y, et al. (2004) Methylglyoxal induces apoptosis through activation of p38 MAPK in rat Schwann cells. Biochem Biophys Res Commun 320: 689-695.
27. Heimfarth L, Loureiro SO, Pierozan P, de Lima BO, Reis KP, et al. (2013) Methylglyoxal-induced cytotoxicity in neonatal rat brain: a role for oxidative stress and MAP kinases. Metab Brain Dis 28: 429-438.
28. Palsamy P, Bidasee KR, Ayaki M, Augusteyn RC, Chan JY, et al. (2014) Methylglyoxal induces endoplasmic reticulum stress and DNA demethylation

in the Keap1 promoter of human lens epithelial cells and age-related cataracts. Free Radic Biol Med 72: 134-148.

29. Nam DH, Han JH, Lee TJ, Shishido T, Lim JH, et al. (2015) CHOP deficiency prevents methylglyoxal-induced myocyte apoptosis and cardiac dysfunction. J Mol Cell Cardiol 85: 168-177.

30. Wu J, Kaufman RJ (2006) From acute ER stress to physiological roles of the Unfolded Protein Response. Cell Death Differ 13: 374-384.

31. Karali E, Bellou S, Stellas D, Klinakis A, Murphy C, et al. (2014) VEGF Signals through ATF6 and PERK to promote endothelial cell survival and angiogenesis in the absence of ER stress. Mol Cell 54: 559-572.

32. Morishima N, Nakanishi K, Nakano A (2011) Activating transcription factor-6 (ATF6) mediates apoptosis with reduction of myeloid cell leukemia sequence 1 (Mcl-1) protein via induction of WW domain binding protein 1. J Biol Chem 286: 35227-35235.

33. Yoshida H, Okada T, Haze K, Yanagi H, Yura T, et al. (2000) ATF6 activated by proteolysis binds in the presence of NF-Y (CBF) directly to the cis-acting element responsible for the mammalian unfolded protein response. Mol Cell Biol 20: 6755-6767.

34. Chan CM, Huang DY, Huang YP, Hau SH, Kang LY, et al. (2016) Methylglyoxal induces cell death through endoplasmic reticulum stress-associated ROS production and mitochondrial dysfunction. J Cell Mol Med.